

## Failure life estimation of sharp-notched circular tubes with different notch depths under cyclic bending

Kuo-Long Lee<sup>1a</sup>, Kao-Hua Chang<sup>2b</sup> and Wen-Fung Pan<sup>\*3</sup>

<sup>1</sup>*Department of Innovative Design and Entrepreneurship Management, Far East University, No. 49, Chung Hua Rd., Hsin-Shih Dist., Tainan 744, Taiwan*

<sup>2</sup>*Department of Mold and Die Engineering, National Kaohsiung University of Applied Sciences, No. 415, Chien Kung Rd., Kaohsiung 807, Taiwan*

<sup>3</sup>*Department of Engineering Science, National Cheng Kung University, No. 1, University Rd., Tainan 701, Taiwan*

*(Received November 8, 2015, Revised July 26, 2016, Accepted July 29, 2016)*

**Abstract.** In this paper, the response and failure of sharp-notched 6061-T6 aluminum alloy circular tubes with five different notch depths of 0.4, 0.8, 1.2, 1.6 and 2.0 mm subjected to cyclic bending were experimentally and theoretically investigated. The experimental moment-curvature relationship exhibits an almost steady loop from the beginning of the first cycle. And, the notch depth has almost no influence on its relationship. However, the ovalization-curvature relationship exhibits a symmetrical, increasing, and ratcheting behavior as the number of cycles increases. In addition, a higher notch depth of a tube leads to a more severe unsymmetrical trend of the ovalization-curvature relationship. Focusing on the aforementioned relationships, the finite element software ANSYS was used to continue the related theoretical simulation. Furthermore, the five groups of tubes tested have different notch depths, from which five unparallel straight lines can be observed from the relationship between the controlled curvature and the number of cycles required to produce failure in the log-log scale. Finally, a failure model was proposed to simulate the aforementioned relationship. Through comparison with the experimental data, the proposed model can properly simulate the experimental data.

**Keywords:** failure life estimation; sharp-notched circular tubes; cyclic bending; moment; curvature; ovalization; finite element ANSYS analysis

### 1. Introduction

It is well known that the bending of circular tubes results in the ovalization (change in the outer diameter divided by the original outer diameter) of the tube cross-section. This ovalization increases slowly during reverse bending and continuous cyclic bending and, in turn, results in the deterioration of the circular tube, which buckles or fractures when the ovalization reaches some critical value. The circular tube is severely damaged during buckling or cracking and cannot bear

---

\*Corresponding author, Professor, E-mail: [z788034@email.ncku.edu.tw](mailto:z788034@email.ncku.edu.tw)

<sup>a</sup>Professor, E-mail: [lkl@cc.feu.edu.tw](mailto:lkl@cc.feu.edu.tw)

<sup>b</sup>Associate Professor, E-mail: [kfchuang@kuas.edu.tw](mailto:kfchuang@kuas.edu.tw)

the load, which ultimately results in obstruction and leakage of the material being transported. As such, a complete understanding of the response of the circular tube under cyclic bending is essential for industrial applications.

As part of the earliest research regarding this issue, Kyriakides *et al.* designed and constructed a tube cyclic bending machine and conducted a series of experimental and theoretical investigations. Shaw and Kyriakides (1985) later investigated the inelastic behavior of tubes subjected to cyclic bending and extended the analysis of tubes to stability conditions under cyclic bending (Kyriakides and Shaw 1987). Corona and Kyriakides (1988) investigated the stability of tubes subjected to combined bending and external pressure; they also later (Corona and Kyriakides 1991) studied the degradation and buckling of tubes under cyclic bending and external pressure. Corona and Vaze (1996) studied the response, buckling, and collapse of long, thin-walled seamless steel square tubes under bending, and later Vaze and Corona (1998) experimentally investigated the elastic-plastic degradation and collapse of steel tubes with square cross-sections under cyclic bending. Corona and Kyriakides (2000) also studied the asymmetric collapse modes of pipes under combined bending and pressure. Corona, Lee *et al.* (2006) conducted a set of bending experiments on aluminum alloy tubes to investigate the yield anisotropy effects on buckling. Later, Kyriakides, Ok *et al.* (2008) studied the plastic bending of steel tubes with a diameter-to-thickness ratio ( $D_o/t$  ratio) of 18.8, exhibiting Lüders bands through the experiment. Limam, Lee *et al.* (2010) studied the inelastic bending and collapse of tubes in the presence of bending and internal pressure. Hallai and Kyriakides (2011) experimentally studied the effect of Lüders bands on the bending of steel tubes. Limam, Lee *et al.* (2012) investigated the collapse of dented tubes under combined bending and internal pressure. Bechle and Kyriakides (2014) later studied the localization of NiTi tubes subjected to bending.

Additionally, other scholars have published a number of related studies. Yuan and Mirmiran (2001) analytically and experimentally studied the static buckling of thin-walled fiber-reinforced plastic tubes filled with concrete and bent in a single curvature. Elchalakani, Zhao *et al.* (2002) experimentally conducted tests on different  $D_o/t$  ratios of grade C350 steel tubes under pure bending and proposed two theoretical simulation models. Jiao and Zhao (2004) tested the bending behavior of very high strength circular steel tubes and proposed a plastic slenderness limit. Corradi, Luzzi *et al.* (2005) investigated the imperfection sensitivity of cylindrical shells under external pressure. Houliara and Karamanos (2006) investigated the buckling and post-buckling of long-pressurized, elastic, thin-walled tubes under in-phase bending. Elchalakani, Zhao *et al.* (2006) conducted the variable amplitude, cyclic, pure bending tests to determine fully ductile section slenderness limits for cold-formed CHS. Mathon and Liman (2006) experimentally studied the collapse of thin, cylindrical shells that were submitted to internal pressure and pure bending. Elchalakani and Zhao (2008) investigated concrete-filled, cold-formed circular steel tubes that were subjected to variable amplitude, cyclic, pure bending. Fatemi, Kenny *et al.* (2009) discussed the parameters that affect the buckling and post-buckling behavior of high strength pipelines under bending. Suzuki, Tajika *et al.* (2010) researched the local buckling behavior of 48 high-strain line pipes under bending. Yazdani and Nayebi (2013) discussed the ratcheting and fatigue damage of thin-walled tubes under cyclic bending and steady internal pressure. Guo, Yang *et al.* (2013) investigated the behavior of thin-walled circular hollow tubes subjected to bending. Shariati, Kolasangiani *et al.* (2014) experimentally studied the SS316L cantilevered cylindrical shells under cyclic bending loads.

In 1998, Pan, Wang *et al.* (1998) designed and set up a new measurement apparatus. It was used with the cyclic bending machine to study various kinds of tubes under different cyclic

bending conditions. For instance, Pan and Her (1998) investigated the response and stability of circular tubes that were subjected to cyclic bending with different curvature-rates, Lee, Pan *et al.* (2001) studied the influence of the  $D_o/t$  ratio on the response and stability of circular tubes that were subjected to symmetrical cyclic bending, Lee, Pan *et al.* (2004) experimentally explored the effect of the  $D_o/t$  ratio and curvature-rate on the response and stability of circular tubes subjected to cyclic bending, Chang, Pan *et al.* (2008) studied the influence of the mean moment effect on circular, thin-walled tubes under cyclic bending, and Chang and Pan (2009) discussed the buckling life estimation of circular tubes subjected to cyclic bending.

In practical industrial applications, tubes are under the hostile environment, so the material in the environment may corrode the tube surface and produce notches. Additionally, a tube in the working condition often involves some notches. The mechanical behavior and buckling failure of a notched tube differs from that of a tube with a smooth surface. In 2010, Lee, Hung *et al.* (2010) studied the variation in ovalization of sharp-notched circular tubes subjected to cyclic bending. Lee (2010) investigated the mechanical behavior and buckling failure of sharp-notched circular tubes under cyclic bending. Lee, Hsu *et al.* (2013) experimentally discussed the viscoplastic response and collapse of sharp-notched circular tubes subjected to cyclic bending. Later, Lee, Hsu *et al.* (2014) investigated the response of SUS304 stainless steel tubes subjected to pure bending creep and pure bending relaxation.

However, all investigations of the sharp notch were the circumferential sharp notch as shown in Fig. 1. If the sharp notch is a local sharp notch in Fig. 2, the response of a local sharp-notched circular tube under cyclic bending should be different from that of a circumferential sharp-notched circular tube under cyclic bending. Therefore, Lee, Hsu *et al.* (2013) investigated the response of

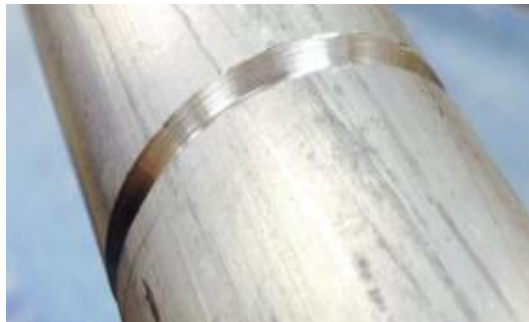


Fig. 1 A picture of the circumferential sharp-notched circular tube



Fig. 2 A picture of the local sharp-notched circular tube

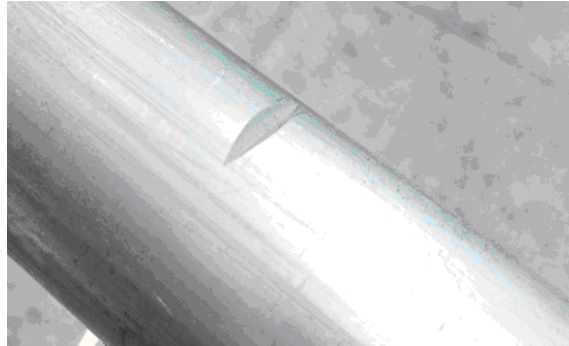


Fig. 3 A picture of the sharp-notched circular tube

local sharp-notched circular tubes with different notch depths subjected to cyclic bending. Later, Lee, Chung *et al.* (2016) studied the influence of the notch direction on the response of local sharp-notched circular tubes under cyclic bending.

It is known that the tubes may be damaged by a sharp object during the delivery, installation or use. Once a notch is on a tube (Fig. 3), the response and failure of the sharp-notched circular tube under cyclic bending should be different from that of a smooth tube or a circular tube with a different type of notch under cyclic bending. Therefore, the response and failure of sharp-notched circular tubes with different notch depths under cyclic bending was investigated in this paper.

For the experimental aspect, a four-point bending machine and curvature-ovalization measurement apparatus (COMA), which were previously designed and reported by Pan, Wang *et al.* (1998), will be adopted to conduct the experiments on the sharp-notched 6061-T6 aluminum alloy circular tubes under cyclic bending. The magnitude of the bending moment will be measured by two load cells mounted in the bending device, and the magnitude of the curvature and ovalization of the tube cross-section by COMA. The number of cycles required to produce failure will be recorded. For the theoretical aspect, the finite element software ANSYS will be used to simulate the moment-curvature and ovalization-curvature relationships. In addition, a theoretical model will be proposed for simulating the controlled curvature-number of cycles required to produce failure.

## 2. Experiments

Sharp-notched 6061-T6 aluminum alloy circular tubes with five different notch depths were subjected to cyclic bending by using a tube-bending device and a curvature ovalization measurement apparatus. Detailed descriptions of the device, apparatus, material, specimens, and test procedures are given in the following subsection.

### 2.1 Tube-bending device

A schematic drawing of the bending device is shown in Fig. 4. The device is designed as a four-point bending machine, capable of applying reverse cyclic bending. The device consists of two rotating sprockets resting on two support beams. Heavy chains run around the sprockets resting on two heavy support beams 1.25 m apart. This allows for a maximum length of 1 m for the test

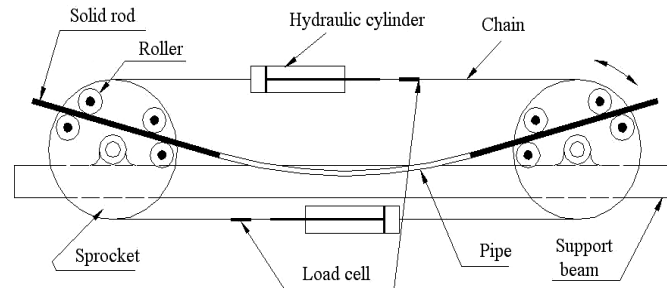


Fig. 4 A schematic drawing of the tube-bending device

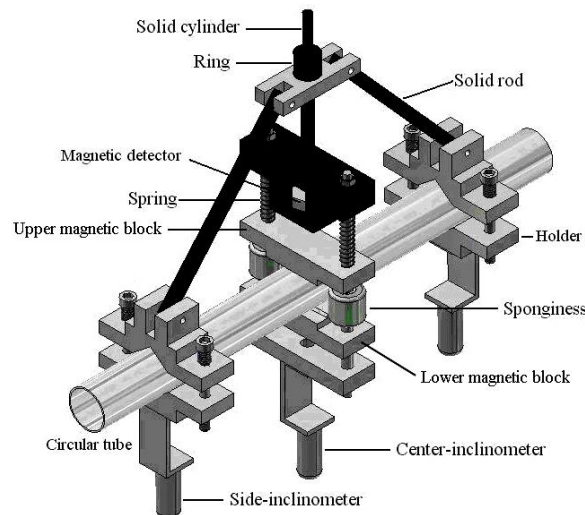


Fig. 5 A schematic drawing of the COMA

specimen. The bending capacity of the machine is 5300 N-m. Each tested tube is fitted with solid rod extensions that engage the rollers. The rods can be freely moved along the axial direction during bending. Once either the top or bottom cylinder is contracted, the sprockets rotate, and bending of the test specimen is achieved. Reverse bending can be achieved by reversing the flow direction in the hydraulic circuit. Detailed description of the bending device can be found in Shaw and Kyriakides (1985) and Pan, Wang *et al.* (1998).

## 2.2 Curvature-ovalization measurement apparatus (COMA)

The COMA, shown schematically in Fig. 5, is an instrument used to measure the tube curvature and ovalization of a tube cross-section. It is a lightweight instrument, which is mounted close to the tube mid-span. There are three inclinometers in the COMA. Two inclinometers are fixed on two holders, which are denoted as side-inclinometers (see Fig. 5). These holders are fixed on the circular tube before the test begins. From the fixed distance between the two side-inclinometers and the angle change detected by the two side-inclinometers, the tube curvature can be derived. In addition, a magnetic detector in the middle part of the COMA is used to measure the change in the

Table 1 Chemical composition of 6161-T6 aluminum alloy

Chemical Composition	Al	Mg	Si	Cu	Ti	Fe
Proportion (%)	97.40	0.916	0.733	0.293	0.268	0.256
Chemical Composition	Mn	Zn	Cr	Ni	Pb	Sn
Proportion (%)	0.132	0.0983	0.0682	0.0056	0.005	<0.001

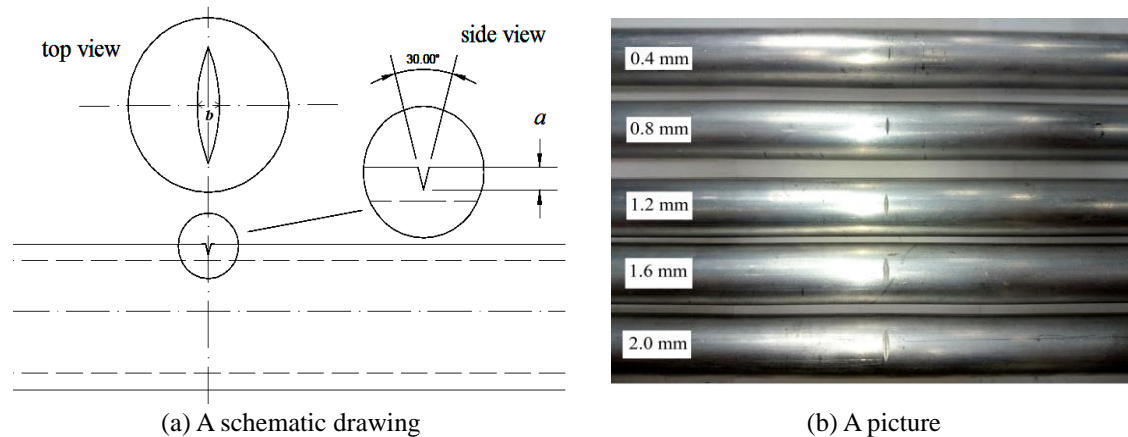


Fig. 6 Tested sharp-notched 6061-T6 aluminum alloy circular tubes

outside diameter. A more detailed description of the bending device and the COMA is given in Pan, Wang *et al.* (1998).

### 2.3 Material and specimens

Circular tubes made of 6061-T6 aluminum alloy were adopted in this study. Table 1 shows the alloy's chemical composition in weight percentage. The ultimate stress is 258 MPa, the 0.2% strain offsetting yield stress is 166 MPa, and the percent elongation is 23%.

The raw, unnotched 6061-T6 aluminum alloy circular tubes had a length  $L_0$  of 500 mm, an outside diameter  $D_0$  of 35.0 mm and a wall thickness  $t$  of 3.0 mm. The raw tubes were machined on the outside surface to obtain the desired shape and depth of the notch. Fig. 6(a) shows a schematic drawing of the sharp-notched circular tube, where the notch depth is denoted as  $a$ . In this study, five different notch depths were considered: 0.4, 0.8, 1.2, 1.6, and 2.0 mm. According to the shape and size of the lathe's cutting knife, the largest notch widths ( $b$ ) at the tube's surface were 0.19, 0.38, 0.57, 0.76, and 0.95 mm, respectively. The notch root radius for all tested tubes was controlled to be less than 1/100 mm and all tested tubes were carefully examined before the test. Fig. 6(b) shows a picture of the tested 6061-T6 aluminum alloy circular tubes with different notch depths. The bending moment, tube's curvature and notch depth were normalized by  $M_0 = \sigma_0 D_0^2 t$ ,  $\kappa_0 = t/D_0^2$  (Corona and Kyriakides 1988) and  $t$ , respectively.

### 2.4 Test procedures

The test involved a curvature-controlled cyclic bending. The controlled-curvature ranges were

from  $\pm 0.2$  to  $\pm 1.1 \text{ m}^{-1}$ , and the curvature-rate of the cyclic bending test was  $0.035 \text{ m}^{-1}\text{s}^{-1}$ . The magnitude of the bending moment was measured by two load cells mounted to the bending device. The magnitude of the curvature and ovalization of the tube cross-section were controlled and measured by the COMA. In addition, the number of cycles required to produce failure was recorded.

### 3. Finite element “ANSYS” analysis

Finite element software ANSYS was used to simulate the response of sharp-notched circular tubes subjected to cyclic bending. The tubes’ response was expressed in terms of the relationships between moment, curvature, and ovalization. The elastoplastic stress-strain relationship, the ANSYS elements, model, boundary and loading conditions are discussed in the following subsections.

#### 3.1 Elastoplastic stress-strain relationship

In this study, the “isotropic elasticity” and “multilinear kinematic hardening” were selected in ANSYS as shown in Fig. 7 for constructing the cyclic uniaxial stress-strain curve. Firstly, the elastic modulus of 68.95 GPa and Poisson’s ratio of 0.33 were entered on the input interface of the “isotropic elasticity”. Then, fourteen uniaxial stress-strain data according to the tested data in Fig. 8(a) were entered on the input interface of the “multilinear kinematic hardening” as shown in the upper right side of Fig. 7. Thus, the stress-strain curve at the initial loading stage was constructed by ANSYS as shown in the lower right side of Fig. 7. The built-in hardening rule in the “multilinear kinematic hardening” is just the basic kinematic hardening rule. The cyclic uniaxial stress-strain curve for 6061-T6 aluminum alloy was automatically constructed in ANSYS as shown in Fig. 8(b). In addition, other material parameters that must be entered include the density of  $2712.6 \text{ kg/m}^3$  and ultimate stress of 258 MPa.

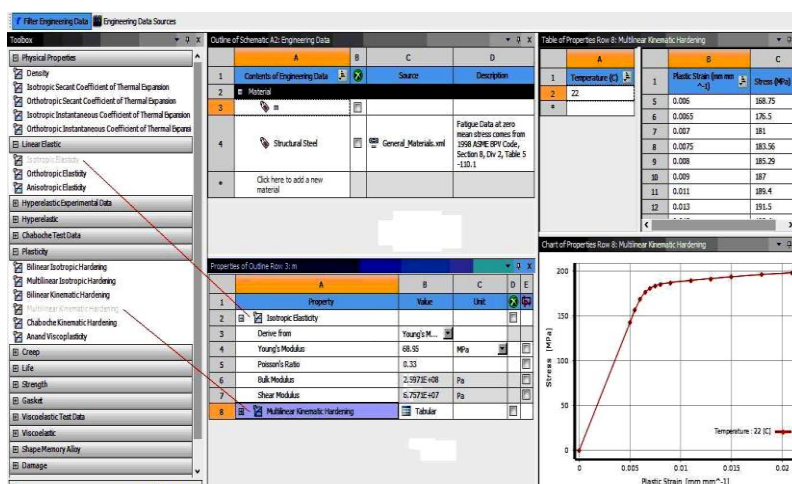
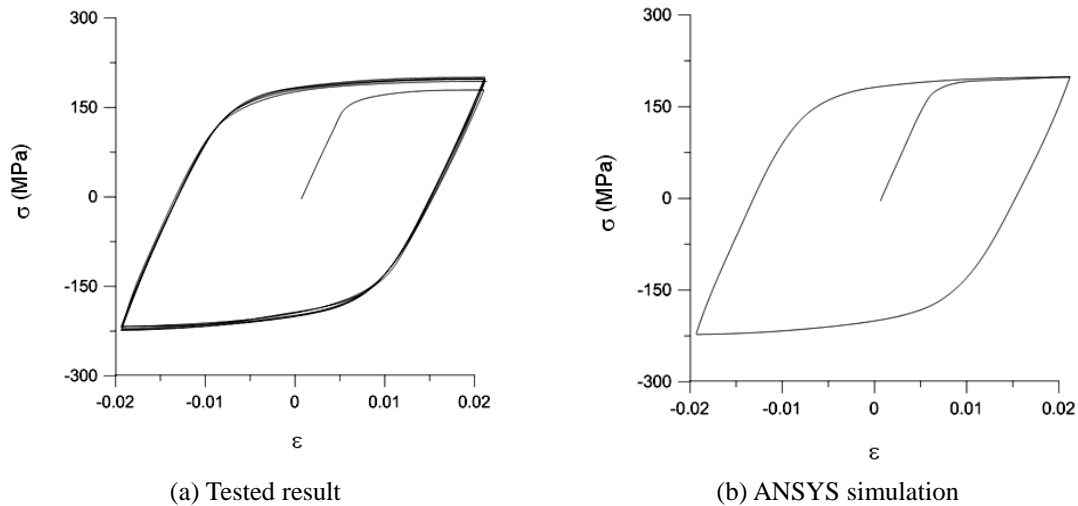


Fig. 7 Screenshot of the input interface of the uniaxial stress-strain curve for 6061-T6 aluminum alloy in ANSYS



(a) Tested result

(b) ANSYS simulation

Fig. 8 Uniaxial cyclic stress-strain curve for 6061-T6 aluminum alloy

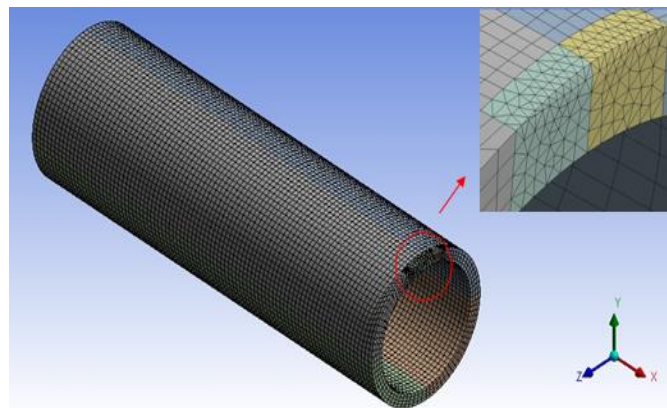


Fig. 9 Mesh constructed by ANSYS for half tube

### 3.2 Element and model of ANSYS

Due to the three-dimensional geometry and elastoplastic deformation of the tube, the SOLID 186 element was used in the related analysis. This element is a tetrahedral element built in ANSYS and is suitable for analyzing plastic and large deformations. In particular, this element is adequate for analysis of shell components under bending. Due to the symmetry of the tube's left/right quarter, only half of the tube's model was constructed. Fig. 9 shows the mesh constructed by ANSYS for half tube.

### 3.3 Boundary and loading conditions

Fig. 10(a) shows the restrictions on the symmetrical plane (central cross-section), constructed by ANSYS for a tube subjected to cyclic bending. Since the tubes were bent in the  $z$ -direction only,

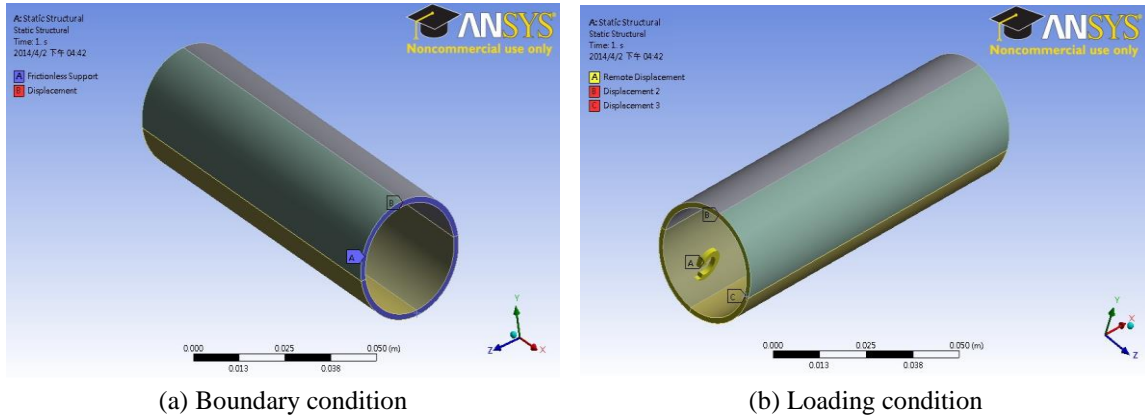


Fig. 10 Boundary and loading conditions constructed by ANSYS

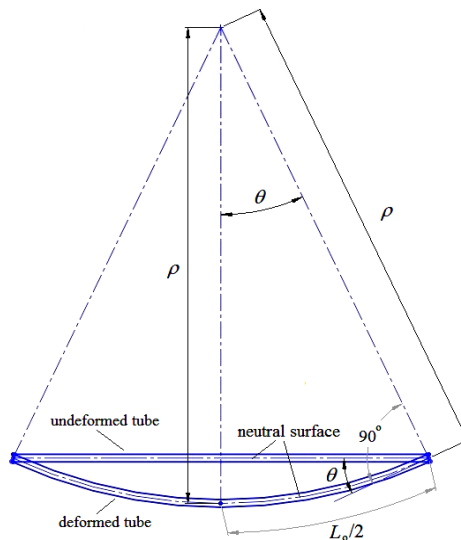


Fig. 11 Relationship between rotating angle  $\theta$  and curvature  $\kappa$  for a tube under pure bending

the frictionless roller support was fixed to the symmetrical plane and the displacement in the  $z$ -direction of this plane was set to zero. Fig. 10(b) shows the loading condition constructed by ANSYS on the basis of the tube bending device. As the figure shows, the remote displacement in the  $z$ -direction was unrestricted, i.e., the rotation was free to move in the  $z$ -direction. In addition, the bending moment was applied only in the  $z$ -direction and hence, the rotations in the  $x$ - and  $y$ -directions were set to zero.

The rotating angle  $\theta$  in the  $z$ -direction (Fig. 11) was used as the input data (loading condition) for the tube under curvature-controlled cyclic bending. The relationship between  $\theta$  and curvature  $\kappa$  is

$$\kappa = 1 / \rho = 2\theta / L_0 \tag{1}$$

where  $L_0$  is the original tube length.

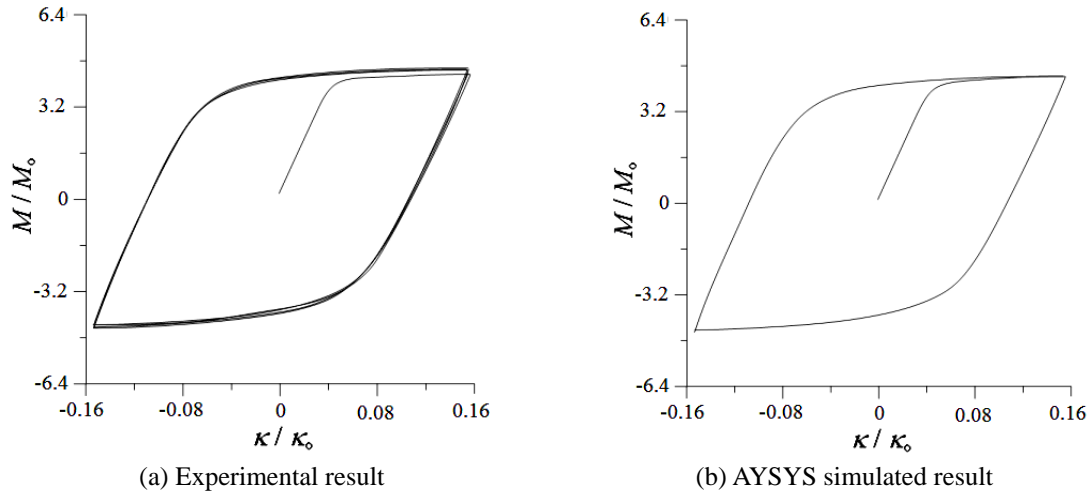


Fig. 12 Moment ( $M/M_0$ ) - curvature ( $\kappa/\kappa_0$ ) curves for sharp-notched 6061-T6 aluminum alloy circular tube with  $a=0.4$  mm under cyclic bending

#### 4. Response of sharp-notched 6061-T6 aluminum alloy tubes under cyclic bending

Fig. 12(a) shows a typical set of experimentally determined cyclic moment ( $M/M_0$ ) - curvature ( $\kappa/\kappa_0$ ) curves for sharp-notched 6061-T6 aluminum alloy circular tubes, with notch depth of  $a=0.4$  mm, subjected to cyclic bending. The tubes were cycled between  $\kappa/\kappa_0=\pm 0.16$ . It was observed that the  $M/M_0$ - $\kappa/\kappa_0$  relationship was linear for a small curvature. However, it became nonlinear for a large curvature. In addition, the  $M/M_0$ - $\kappa/\kappa_0$  response was seen to be characterized by a nearly closed and steady hysteresis loop from the first cycle. Since the sharp notch is small and local, the notch depth has almost no influence on the  $M/M_0$ - $\kappa/\kappa_0$  curve. Therefore, the  $M/M_0$ - $\kappa/\kappa_0$  curves for different values of  $a$  are not shown in this paper. Fig. 12(b) shows the corresponding simulated  $M/M_0$ - $\kappa/\kappa_0$  curve by ANSYS.

Figs. 13(a)-(e) show the experimentally determined ovalization ( $\Delta D_0/D_0$ )-curvature ( $\kappa/\kappa_0$ ) curves for sharp-notched 6061-T6 aluminum alloy circular tubes submitted to cyclic bending; notch depths of  $a=0.4, 0.8, 1.2, 1.6$  and  $2.0$  mm were considered. The ovalization is defined as  $\Delta D_0/D_0$ , where  $D_0$  is the outside diameter and  $\Delta D_0$  is the change in the outside diameter. It can be seen that the ovalization increases in a ratcheting and unsymmetrical manner with the number of bending cycles. A higher value of  $a$  causes greater ovalization in the tube cross-section. In addition, higher values of  $a$  lead to more severe unsymmetrical trend in the  $\Delta D_0/D_0$ - $\kappa/\kappa_0$  curve. This phenomenon of  $\Delta D_0/D_0$ - $\kappa/\kappa_0$  curves is similar to that for local sharp-notched SUS304 stainless steel circular tubes subjected to cyclic bending (Lee, Hsu *et al.* 2013). Because the strength of the 6061-T6 aluminum alloy is weaker than that of the SUS304 stainless steel, the ovalization increments for sharp-notched 6061-T6 aluminum alloy circular tubes become relatively large. In addition, the unsymmetrical trend of  $\Delta D_0/D_0$ - $\kappa/\kappa_0$  curves for sharp-notched 6061-T6 aluminum alloy circular tubes is more significant than that for local sharp-notched SUS304 stainless steel circular tubes. Figs. 14(a)-(e) depict the corresponding simulated  $\Delta D_0/D_0$ - $\kappa/\kappa_0$  curves by ANSYS. The ANSYS simulated results exhibit good correspondence to those obtained from the experiments.

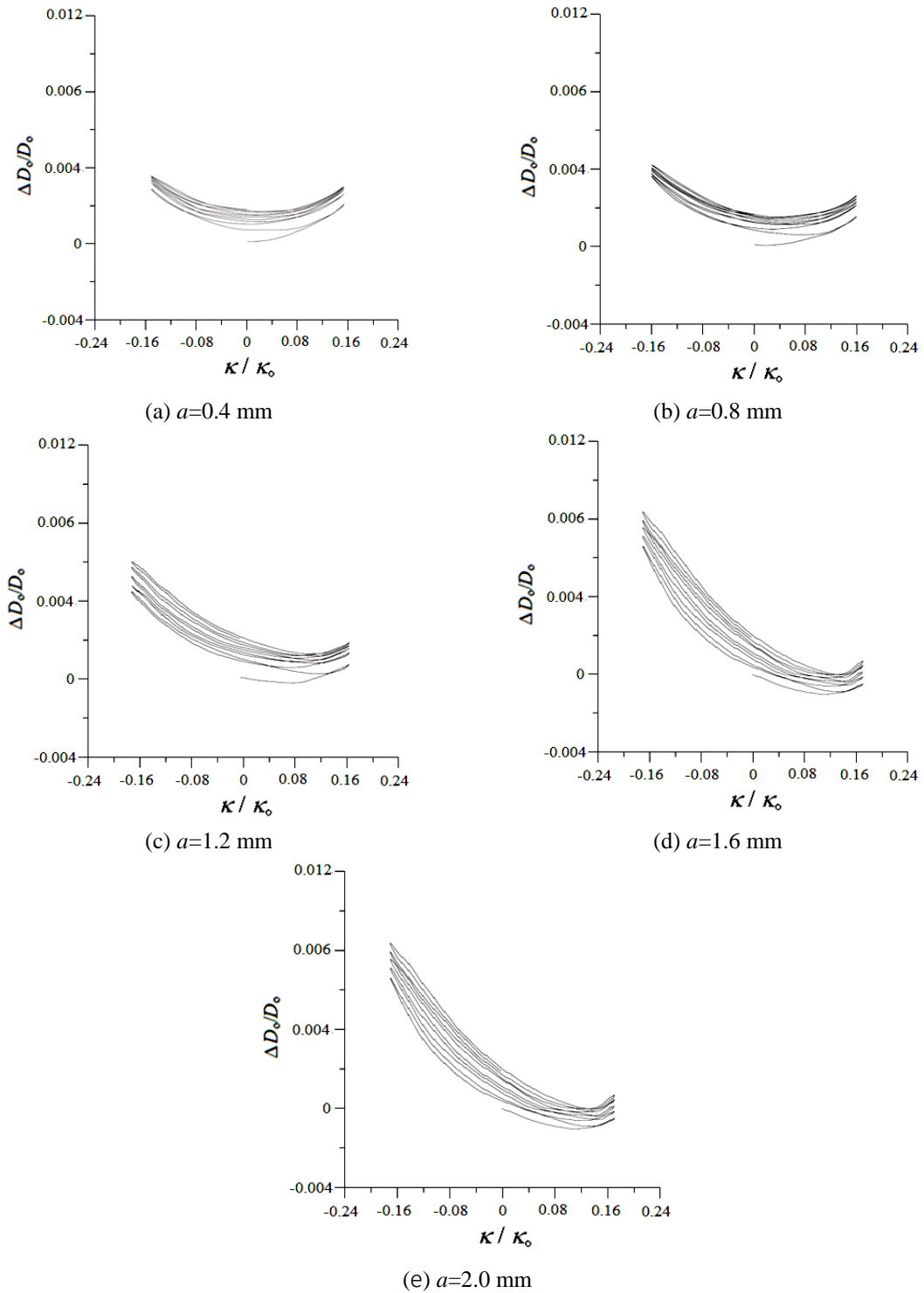


Fig. 13 Experimental ovalization ( $\Delta D_0/D_0$ ) - curvature ( $\kappa/\kappa_0$ ) curves for sharp-notched 6061-T6 aluminum alloy circular tubes with different  $a$  under cyclic bending

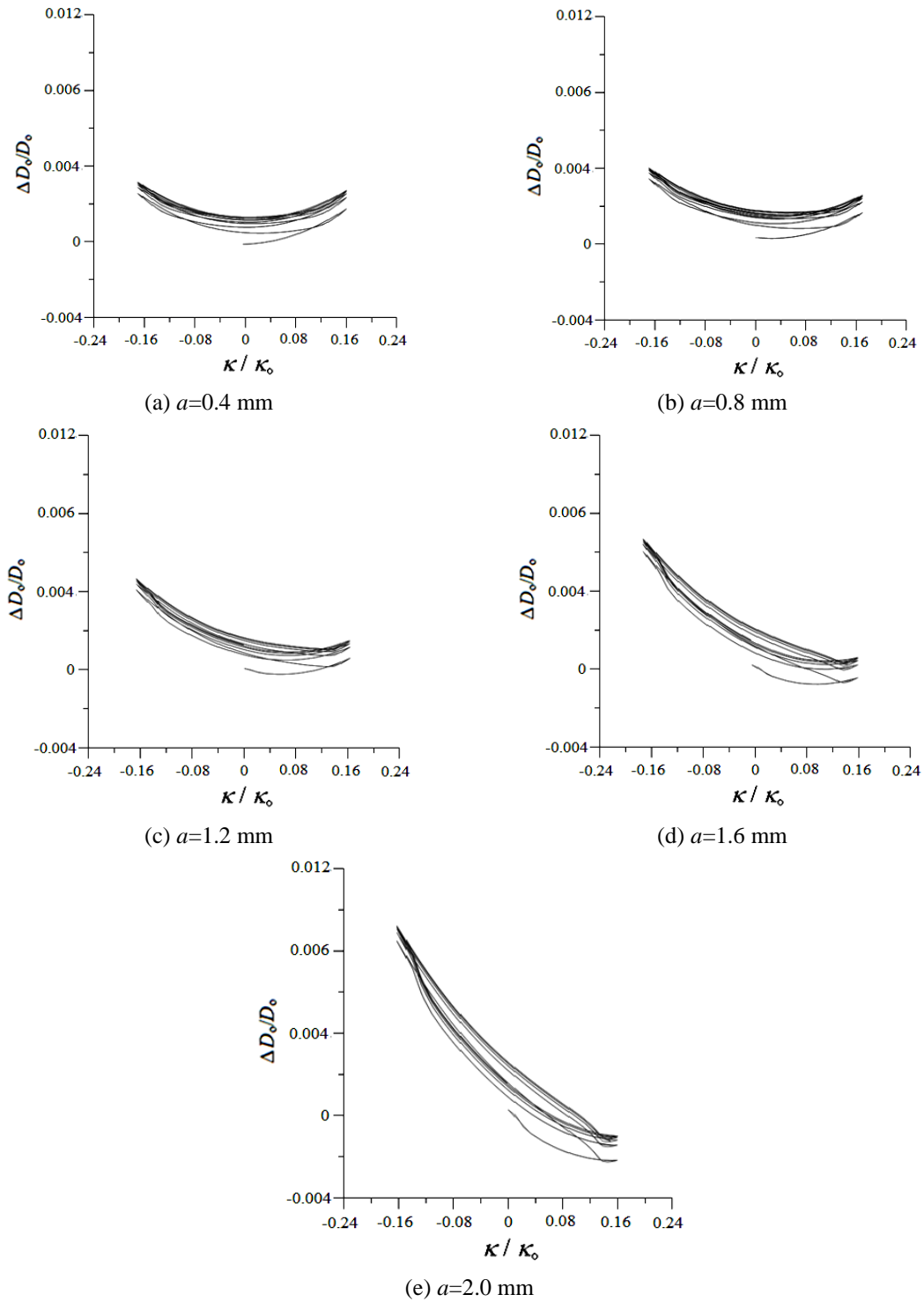


Fig. 14 ANSYS simulated ovalization ( $\Delta D_o/D_o$ ) - curvature ( $\kappa/\kappa_o$ ) curves for sharp-notched 6061-T6 aluminum alloy circular tubes with different  $a$  under cyclic bending

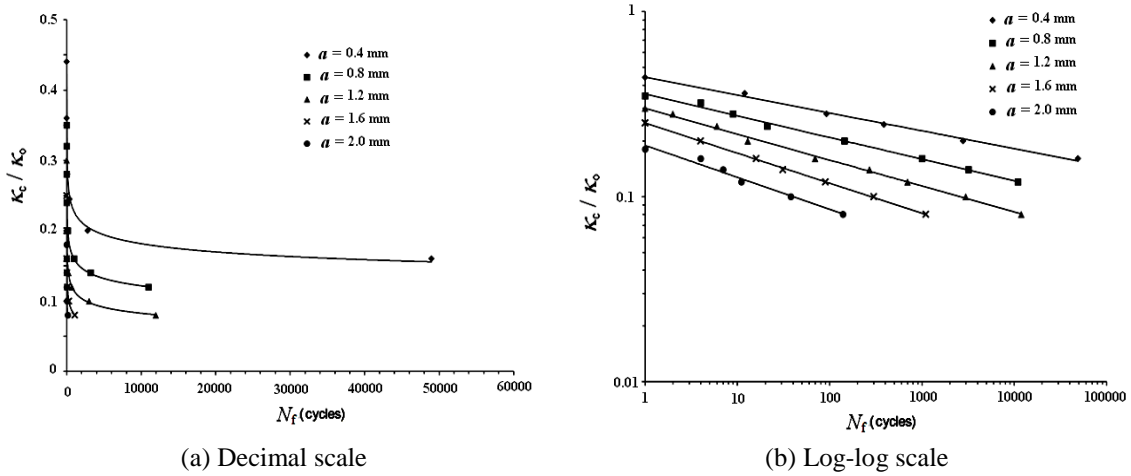


Fig. 15 Experimental controlled curvature ( $\kappa_c/\kappa_0$ ) versus the number of cycles required to produce failure ( $N_f$ ) for sharp-notched 6061-T6 aluminum alloy circular tubes with  $a = 0.4, 0.8, 1.2, 1.6$  and  $2.0$  mm under cyclic bending

### 5. Failure of sharp-notched 6061-T6 aluminum alloy tubes under cyclic bending

Fig. 15(a) shows the experimental results of the controlled curvature ( $\kappa_c/\kappa_0$ ) versus the number of cycles required to produce failure ( $N_f$ ) for sharp-notched 6061-T6 aluminum alloy circular tubes with  $a = 0.4, 0.8, 1.2, 1.6$  and  $2.0$  mm under cyclic bending. It was observed that for a given  $\kappa_c/\kappa_0$ , a tube with a higher value of  $a$  yields a lower  $N_f$ . The experimental results of Fig. 15(a) were plotted on a log-log scale in Fig. 15(b), where the straight lines were determined by the least-squares method. Five unparallel lines can be seen for five different notch depths.

Kyriakides and Shaw (1987) have proposed a formulation of the relationship between  $\kappa_c/\kappa_0$  and  $N_f$  for the material they tested as

$$\kappa_c/\kappa_0 = C (N_f)^{-\alpha} \tag{2}$$

or

$$\log \kappa_c/\kappa_0 = \log C - \alpha \log N_f \tag{3}$$

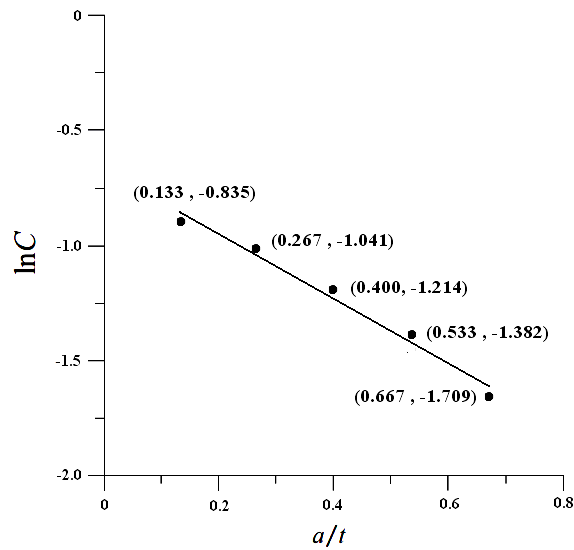
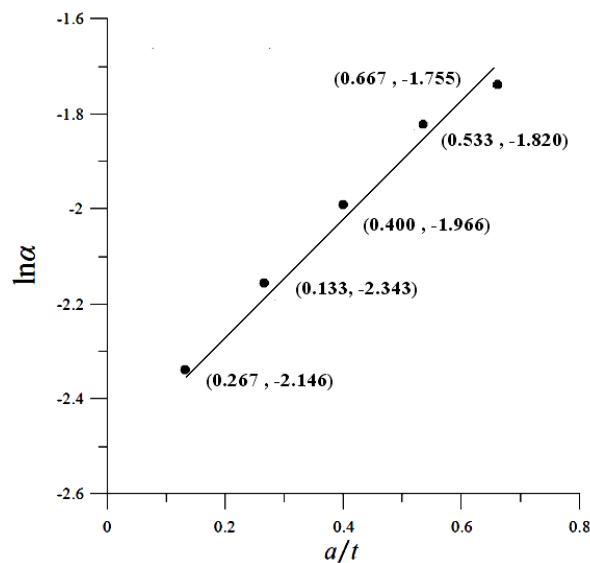
where  $C$  and  $\alpha$  are the material parameters, which are related to the material properties and the  $D_o/t$  ratio. The material parameter  $C$  is the controlled curvature magnitude at  $N_f=1$ , and  $\alpha$  is the slope in the log-log plot. According to the experimental data, five quantities  $C$  of 0.434, 0.353, 0.297, 0.251 and 0.181 and  $\alpha$  of 0.096, 0.117, 0.140, 0.162 and 0.173 can be determined for  $a = 0.4, 0.8, 1.2, 1.6$  and  $2.0$  mm, respectively.

According to the distributions of the relationship between  $\ln C$  and  $a/t$  in Fig. 16 and the relationship between  $\ln \alpha$  and  $a/t$  in Fig. 17, the following formulations were proposed as

$$\ln C = c_1 (a/t) + c_2 \tag{4}$$

and

$$\ln \alpha = d_1 (a/t) + d_2 \tag{5}$$

Fig. 16 Relationship between  $\ln C$  and  $a/t$ Fig. 17 Relationship between  $\ln \alpha$  and  $a/t$ 

where  $c_1$ ,  $c_2$ ,  $d_1$  and  $d_2$  are material parameters. The magnitudes of  $c_1$ ,  $c_2$ ,  $d_1$  and  $d_2$  can be determined to be -1.431, -0.671, 1.237 and -2.522, respectively. Fig. 18 shows the experimental and simulated  $\kappa_c/\kappa_0-N_f$  relationships for sharp-notched 6061-T6 aluminum alloy circular tubes with  $a=0.4, 0.8, 1.2, 1.6$  and  $2.0$  mm under cyclic bending on a log-log scale. Fig. 19 shows a picture of the failure for sharp-notched 6061-T6 aluminum alloy circular tubes with  $a=0.4, 0.8, 1.2, 1.6$  and  $2.0$  mm under cyclic bending. The red circles denote the initiation of the crack. It can be seen that the crack initiates at the one or both sides of the notch. In addition, once the crack initiation is observed, the tube rapidly breaks.

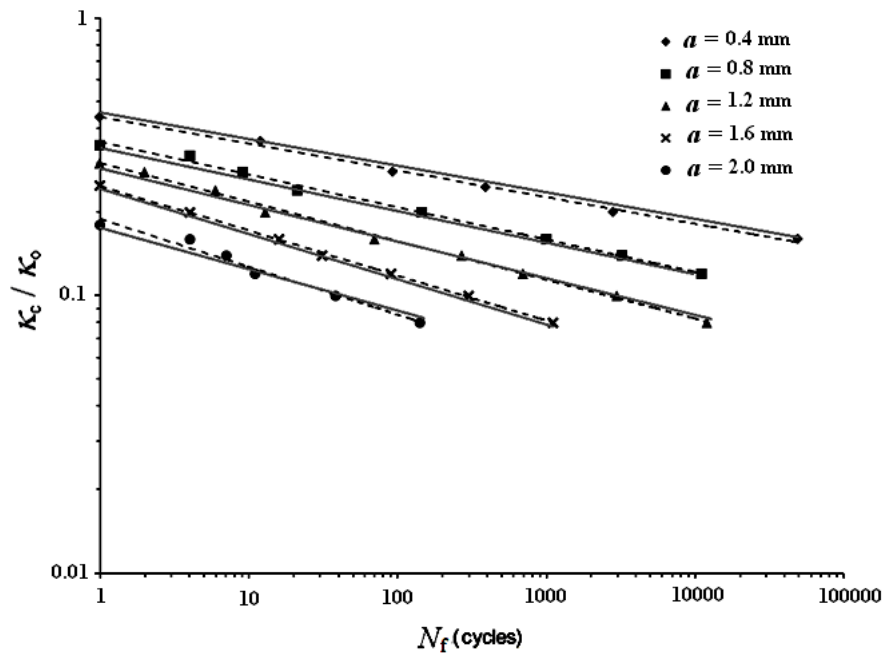


Fig. 18 Experimental and simulated controlled curvature ( $\kappa_c / \kappa_0$ ) versus the number of cycles required to produce failure ( $N_f$ ) for sharp-notched 6061-T6 aluminum alloy circular tubes with  $a = 0.4, 0.8, 1.2, 1.6$  and  $2.0$  mm under cyclic bending on a log-log scale



Fig. 19 A picture of the failure for sharp-notched 6061-T6 aluminum alloy circular tubes with  $a = 0.4, 0.8, 1.2, 1.6$  and  $2.0$  mm under cyclic bending

## 6. Conclusions

The response and failure of sharp-notched 6061-T6 aluminum alloy circular tubes with different notch depths subjected to cyclic bending were investigated in this study. On the basis of the experimental and theoretical results, the following conclusions can be drawn:

- (1) The  $M/M_o-\kappa/\kappa_o$  curves of sharp-notched 6061-T6 aluminum alloy circular tubes with any notch depth exhibit a steady loop from the first cycle under curvature-controlled cyclic bending. In addition, the stable  $M/M_o-\kappa/\kappa_o$  loops have very similar shape and size irrespective of the notch depth.
- (2) The  $\Delta D_o/D_o-\kappa/\kappa_o$  curves of sharp-notched 6061-T6 aluminum alloy circular tubes show that the ovalization of the tube cross-section increases in a ratcheting manner with increasing number of cycles. Higher values of  $a$  lead to more unsymmetrical trends and larger ovalizations of the tube cross-section compared with those obtained at lower values of  $a$ .
- (3) Using adequate stress-strain relationships, mesh, boundary conditions, and loading conditions, the finite element software ANSYS can simulate the behavior of sharp-notched circular tubes subjected to cyclic bending; this behavior includes the  $M/M_o-\kappa/\kappa_o$  and  $\Delta D_o/D_o-\kappa/\kappa_o$  relationships. The simulated results exhibited close correspondence to those obtained from experiments.
- (4) The formulation (Eq. (2)) proposed by Kyriakides and Shaw (1987) was modified for simulating the relationship between  $\kappa_c/\kappa_o$  and  $N_f$  for sharp-notched 6061-T6 aluminum alloy circular tubes with  $a=0.4, 0.8, 1.2, 1.6$  and  $2.0$  mm under cyclic bending. The formulation of the parameters  $C$  and  $\alpha$  were proposed in Eqs. (4) and (5), respectively. It can be seen that the simulation by Eqs. (2), (4) and (5) is in good agreement with the experimental result as shown in Fig. 18.

## Acknowledgments

The work presented was carried out with the support of the National Science Council under grant MOST 104-2221-E-006-111. Its support is gratefully acknowledged.

## References

- Bechle, N.J. and Kyriakides, S. (2014), "Localization of NiTi tubes under bending", *Int. J. Solid. Struct.*, **51**(5), 967-980.
- Chang, K.H. and Pan, W.F. (2009), "Buckling life estimation of circular tubes under cyclic bending", *Int. J. Solid. Struct.*, **46**(2), 254-270.
- Chang, K.H., Pan, W.F. and Lee, K.L. (2008), "Mean moment effect of thin-walled tubes under cyclic bending", *Struct. Eng. Mech.*, **28**(5), 495-514.
- Corona, E. and Kyriakides, S. (1988), "On the collapse of inelastic tubes under combined bending and pressure", *Int. J. Solid. Struct.*, **24**(5), 505-535.
- Corona, E. and Kyriakides, S. (1991), "An experimental investigation of the degradation and buckling of circular tubes under cyclic bending and external pressure", *Thin Wall. Struct.*, **12**(3), 229-263.
- Corona, E. and Kyriakides, S. (2000), "Asymmetric collapse modes of pipes under combined bending and external pressure", *J. Eng. Mech.*, **126**(12), 1232-1239.
- Corona, E. and Vaze, S. (1996), "Buckling of elastic-plastic square tubes under bending", *Int. J. Mech. Sci.*, **38**(7), 753-775.
- Corona, E., Lee, L.H. and Kyriakides, S. (2006), "Yield anisotropic effects on buckling of circular tubes under bending", *Int. J. Solid. Struct.*, **43**(22-23), 7099-7118.
- Corradi, L., Luzzi, L. and Trudi, F. (2005), "Plasticity-instability coupling effects on the collapse of thick tubes", *Int. J. Struct. Stabl. Dyn.*, **5**(1), 1-18.

- Elchalakani M. and Zhao X.L. (2008), "Concrete-filled cold-formed circular steel tubes subjected to variable amplitude cyclic pure bending", *Eng. Struct.*, **30**(2), 287-299.
- Elchalakani, M., Zhao, X.L. and Grzebieta, R.H. (2002), "Plastic mechanism analysis of circular tubes under pure bending", *Int. J. Mech. Sci.*, **44**(6), 1117-1143.
- Elchalakani, M., Zhao, X.L. and Grzebieta, R.H. (2006), "Variable amplitude cyclic pure bending tests to determine fully ductile section slenderness limits for cold-formed CHS", *Eng. Struct.*, **28**(9), 1223-1235.
- Fatemi, A., Kenny, S., Sen, M., Zhou, J., Tahern, F. and Paulin, M. (2009), "Parameters affecting buckling and post-buckling behavior of high strength pipelines", *Proc. of the 28<sup>th</sup> International Conference on Ocean, Offshore Mechanics and Arctic Engineering*, Hawaii, U.S.A., OMAE2009-79578.
- Guo, L., Yang, S. and Jiao, H. (2013), "Behavior of thin-walled circular hollow section tubes subjected to bending", *Thin Wall. Struct.*, **73**, 281-289.
- Hallai, J.F. and Kyriakides, S. (2011), "On the effect of Lüders bands on the bending of steel tubes", *Int. J. Solid. Struct.*, **48**(24), 3275-3284.
- Houliara, S. and Karamanos, S.A. (2006), "Buckling and post-buckling of long pressurized elastic thin-walled tubes under in-plane bending", *Int. J. Nonlin. Mech.*, **41**(4), 491- 511.
- Jiao, H. and Zhao, X.L. (2004), "Section slenderness limits of very high strength circular steel tubes in bending", *Thin Wall. Struct.*, **42**(9), 1257-1271.
- Kyriakides, S. and Shaw, P.K. (1987), "Inelastic buckling of tubes under cyclic loads", *ASME J. Press. Ves. Tech.*, **109**(2), 169-178.
- Kyriakides, S., Ok, A., and Corona, E. (2008), "Localization and propagation of curvature under pure bending in steel tubes with Lüders bands", *Int. J. Solid. Struct.*, **45**(10), 3074 -3087.
- Lee, K.L. (2010), "Mechanical behavior and buckling failure of sharp-notched circular tubes under cyclic bending", *Struct. Eng. Mech.*, **34**(3), 367-376.
- Lee, K.L. Chung, C.C. and Pan, W.F. (2016), "The effect of notch direction on the stability of local sharp-notched circular tubes under cyclic bending", *Int. J. Appl. Mech.* (in press)
- Lee, K.L., Hsu, C.M. and Pan, W.F. (2013), "Viscoplastic collapse of sharp-notched circular tubes under cyclic bending", *Acta Mech. Solida Sinica*, **26**(6), 629-641.
- Lee, K.L., Hsu, C.M. and Pan, W.F. (2014), "Response of sharp-notched circular tubes under bending creep and relaxation", *Mech. Eng. J.*, **1**(2), 1-14.
- Lee, K.L., Hung, C.Y. and Pan, W.F. (2010), "Variation of ovalization for sharp-notched circular tubes under cyclic bending", *J. Mech.*, **26**(3), 403-411.
- Lee, K.L. Meng, C.H. and Pan, W.F. (2014), "The influence of notch depth on the response of local sharp-notched circular tubes under cyclic bending", *J. Appl. Math. Phys.*, **2**(6), 335-341.
- Lee, K.L., Pan, W.F. and Hsu, C.M. (2004), "Experimental and theoretical evaluations of the effect between diameter-to-thickness ratio and curvature-rate on the stability of circular tubes under cyclic bending", *JSME Int. J., Ser. A*, **47**(2), 212-222.
- Lee, K.L., Pan, W.F. and Kuo, J.N. (2001), "The influence of the diameter-to-thickness ratio on the stability of circular tubes under cyclic bending", *Int. J. Solid. Struct.*, **38**(14), 2401-2413.
- Limam, A., Lee, L.H. and Kyriakides, S. (2012), "On the collapse of dented tubes under combined bending and internal pressure", *Int. J. Solid. Struct.*, **55**(1), 1-12.
- Limam, A., Lee, L.H., Corana, E. and Kyriakides, S. (2010), "Inelastic wrinkling and collapse of tubes under combined bending and internal pressure", *Int. J. Mech. Sci.*, **52**(5), 37-47.
- Mathon, C. and Liman, A. (2006), "Experimental collapse of thin cylindrical shells submitted to internal pressure and pure bending", *Thin Wall. Struct.*, **44**(1), 39-50.
- Pan, W.F. and Her, Y.S. (1998), "Viscoplastic collapse of thin-walled tubes under cyclic bending", *ASME J. Eng. Mat. Tech.*, **120**(4), 287-290.
- Pan, W.F., Wang, T.R. and Hsu, C.M. (1998), "A curvature-ovalization measurement apparatus for circular tubes under cyclic bending", *Exp. Mech.*, **38**(2), 99-102.
- Sakakibara, N., Kyriakides, S. and Corona, E. (2008), "Collapse of partially corrodes or worn pipe under external pressure", *Int. J. Mech. Sci.*, **50**(12), 1586-1597.
- Shariati, M., Kolasangiani, K., Norouzi, G. and Shahnavaz, A. (2014), "Experimental study of SS316L

- cantilevered cylindrical shells under cyclic bending load”, *Thin Wall. Struct.*, **82**, 124-131.
- Shaw, P.K. and Kyriakides, S. (1985), “Inelastic analysis of thin-walled tubes under cyclic bending”, *Int. J. Solid. Struct.*, **21**(11), 1073-1110.
- Suzuki, N., Tajika, H., Igi, S., Okatsu, M., Kondo, J. and Arakawa, T. (2010), “Local buckling behavior of 48 high-strain line pipes”, *Proc. of the 8th International Pipeline Conference*, Alberta, Canada, ICP2010-31637.
- Vaze, S. and Corona, E. (1998), “Degradation and collapse of square tubes under cyclic bending”, *Thin Wall. Struct.*, **31**(4), 325-341.
- Yazdani, H. and Nayebi, A. (2013), “Continuum damage mechanics analysis of thin-walled tube under cyclic bending and internal constant pressure”, *Int. J. Appl. Mech.*, **5**(4), 1350038 [20 pages].
- Yuan, W. and Mirmiran, A. (2001), “Buckling analysis of concrete-filled FRP tubes”, *Int. J. Struct. Stabl. Dyn.*, **1**(3), 367-383.